

International Association of Physical Sciences of Oceans
Montreal, Canada, 20-24 July 2009

Mid-Depth Rossby Wave Propagation in the Tropical North Atlantic Observed from Argo Floats

Peter C. Chu
Naval Postgraduate School (NPS)
Leonid Ivanov (NPS)
Oleg Melnichenko (Univ of Hawaii)
N.C. Wells (SOC, UK)

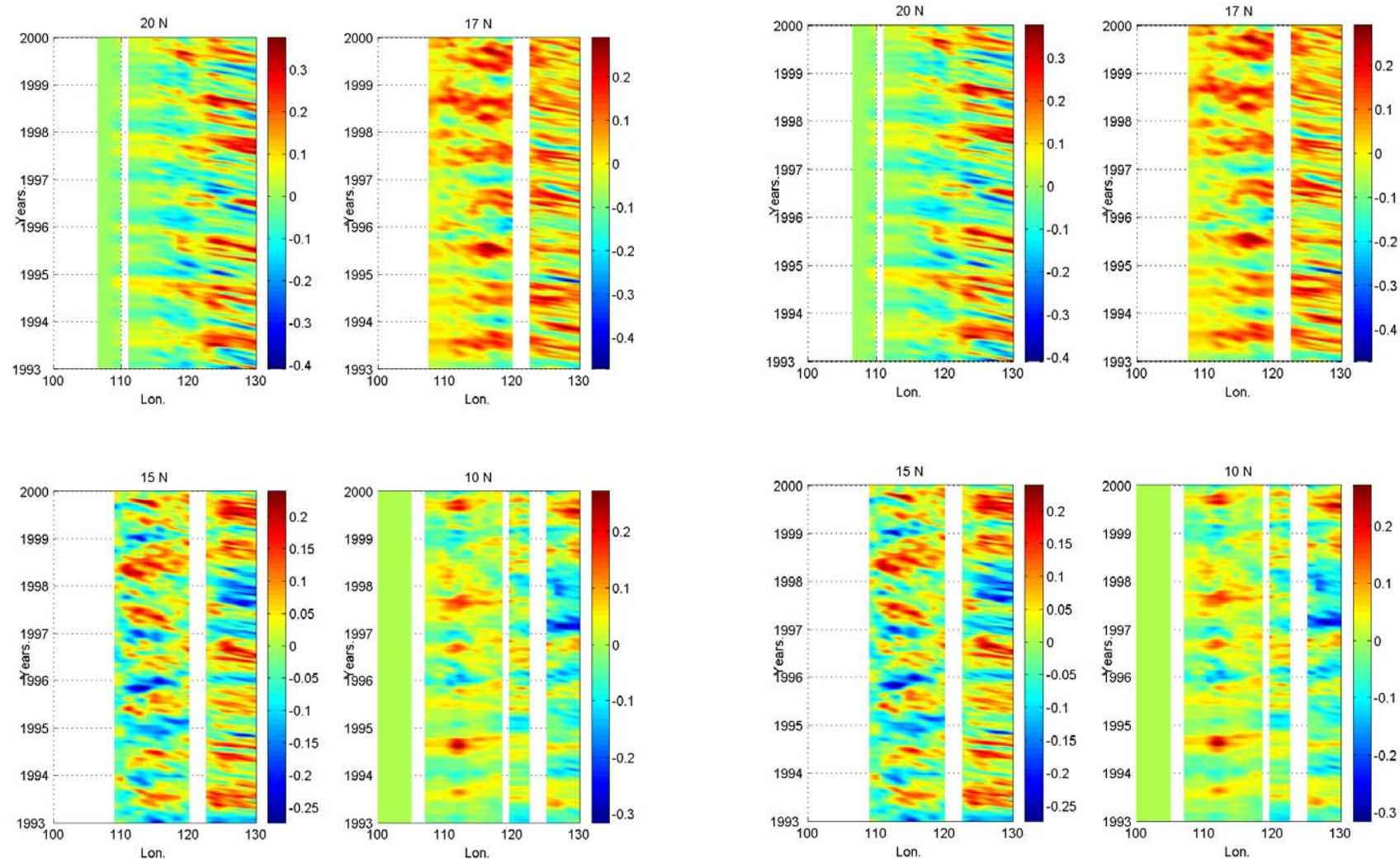
References

- Chu, P.C., L.M. Ivanov, T.P. Korzhova, T.M. Margolina, and O.M. Melnichenko, 2003a: Analysis of sparse and noisy ocean current data using flow decomposition. Part 1: Theory. *Journal of Atmospheric and Oceanic Technology*, 20 (4), 478-491.
- Chu, P.C., L.M. Ivanov, T.P. Korzhova, T.M. Margolina, and O.M. Melnichenko, 2003b: Analysis of sparse and noisy ocean current data using flow decomposition. Part 2: Application to Eulerian and Lagrangian data. *Journal of Atmospheric and Oceanic Technology*, 20 (4), 492-512.
- Chu, P.C., L.M. Ivanov, and T.M. Margolina, 2004: Rotation method for reconstructing process and field from imperfect data. *International Journal of Bifurcation and Chaos*, 14(8), 2991-2997.
- Chu, P.C., L.M. Ivanov, and O.M. Melnichenko, 2005: Fall-winter current reversals on the Texas-Louisiana continental shelf. *Journal of Physical Oceanography*, 35, 902-910
- Chu, P.C., L.M. Ivanov, O.M. Melnichenko, and N.C. Wells, 2007: On long baroclinic Rossby Waves in the tropical North Atlantic observed from profiling floats. *Journal of Geophysical Research – Oceans*, in press.
- These papers can be downloaded from:
- <http://www.oc.nps.navy.mil/~chu>

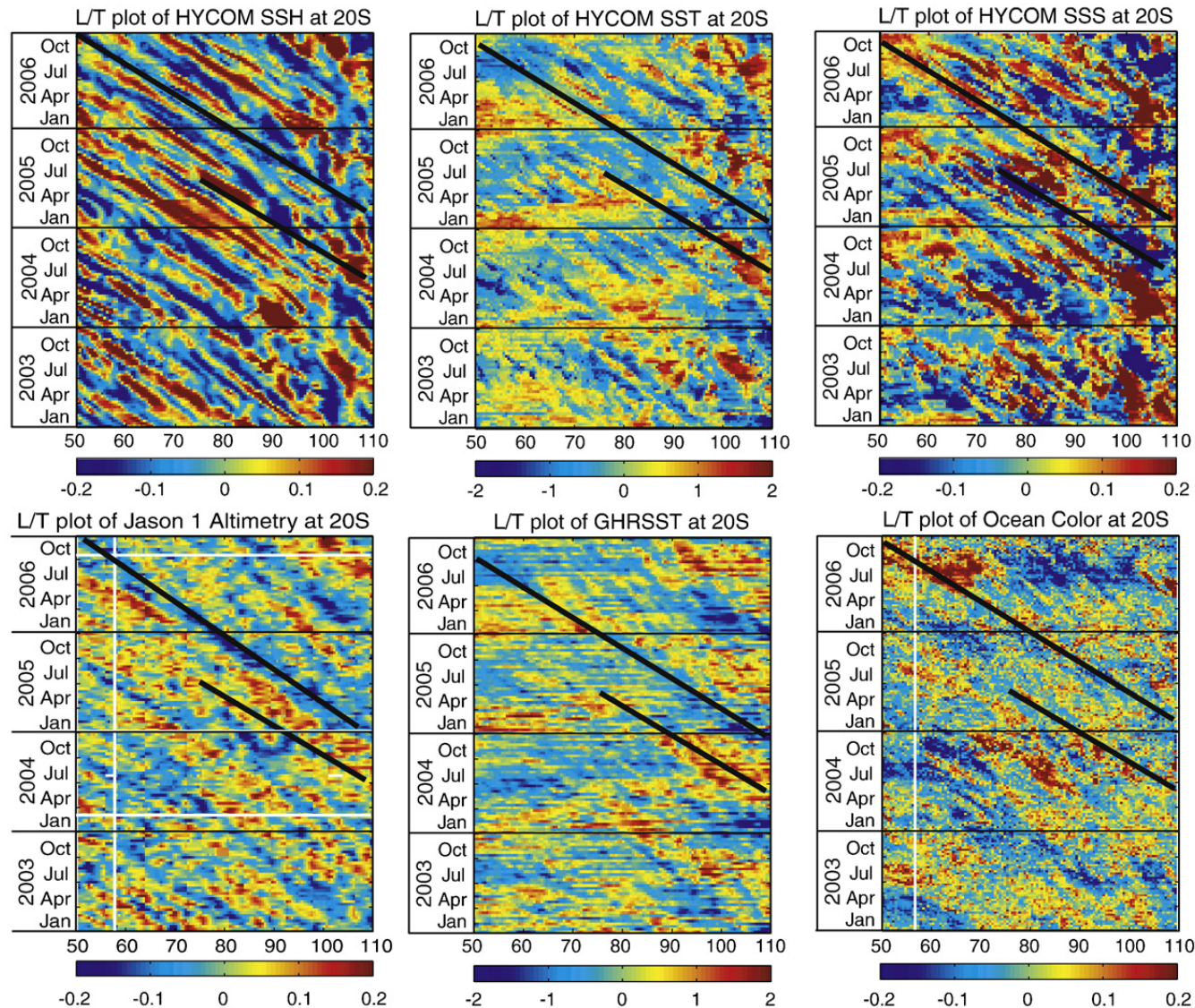
Oceanic Rossby waves have been identified
at the surface from satellite data

- SSH (TOPEX/Poseidon)
- SST
- Ocean Colors

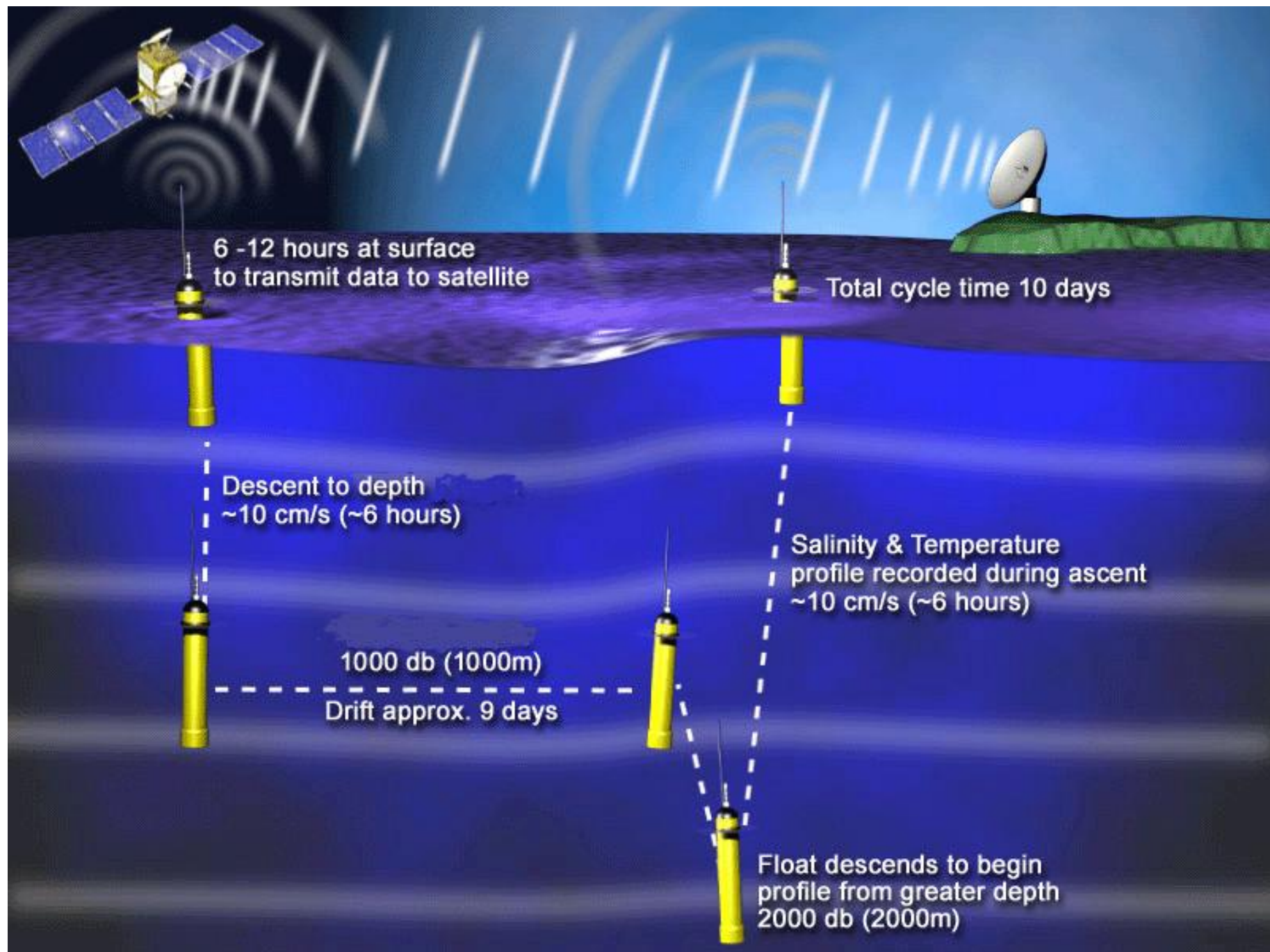
Rossby waves identified from satellite SSH data in the South China Sea (Chu and Fang, 2003)



Rossby waves identified from satellite SST, ocean color data for the Indian Ocean (Subrahmanyam et al. 2009)

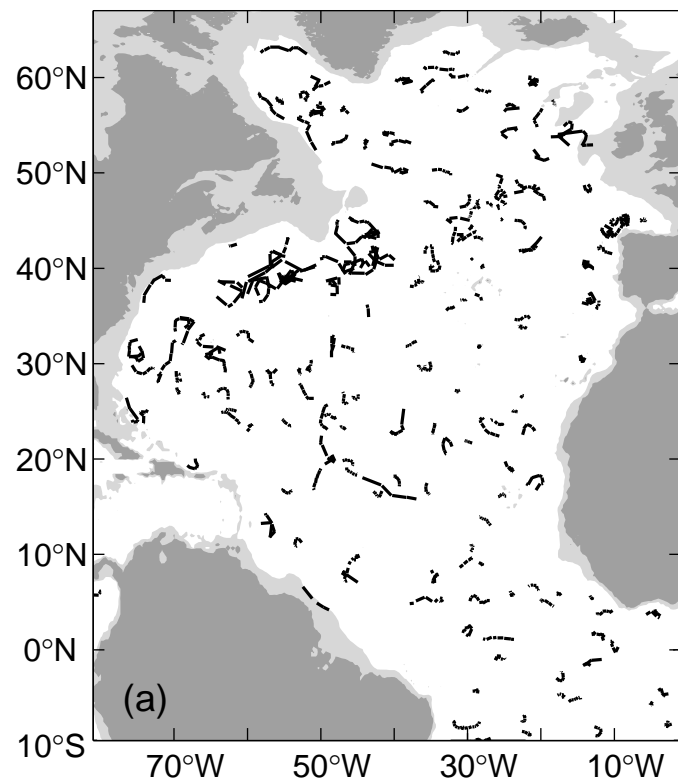


Can we detect the Rossby wave
propagation at the mid-depth
such as 1000 m depth?

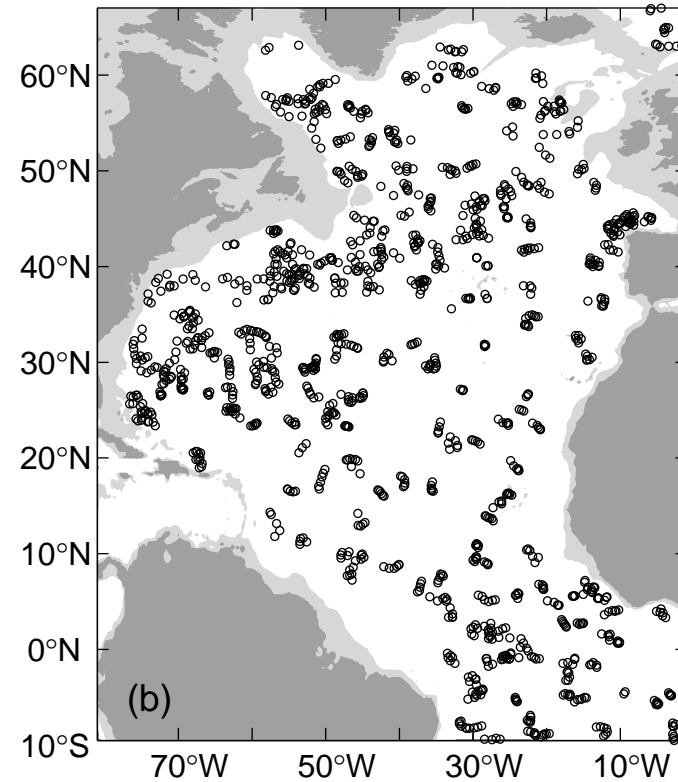


Argo Observations (Oct-Nov 2004)

(a) Subsurface tracks

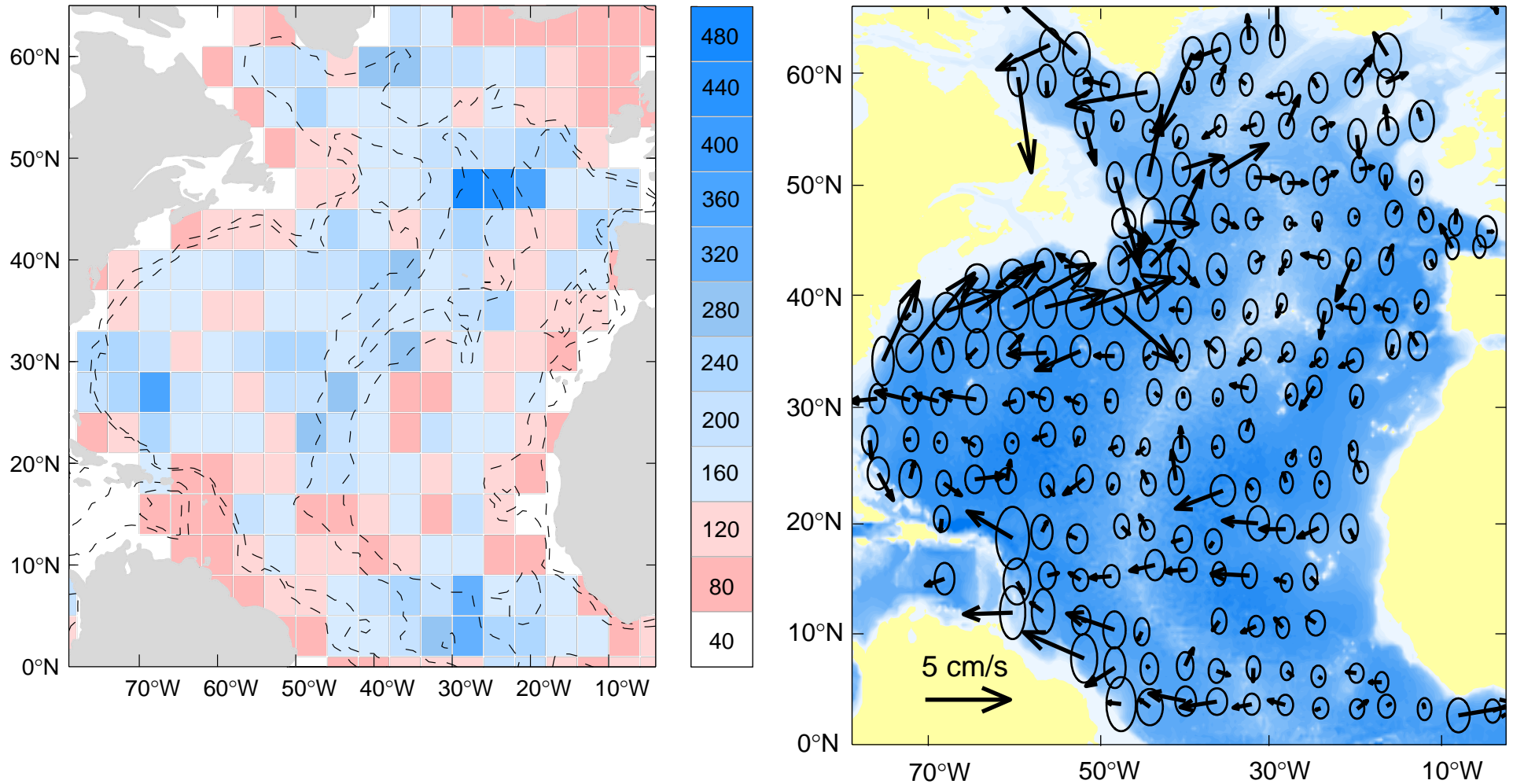


(b) Float positions where (T,S) were measured



Circulations at 1000 m estimated from the original ARGO float tracks (bin method)

April 2004 – April 2005



It is **difficult** to use such noisy data into ocean numerical models.

Optimal Spectral Decomposition (OSD) Method

$$\mathbf{U}_{now}(\mathbf{x}_0, t) = \sum_{s=1}^S a_s(t)[\mathbf{k} \times \nabla Z_s(\mathbf{x}_0)] + \sum_{k=1}^K b_k(t)[\mathbf{k} \times \nabla \Psi_k(\mathbf{x}_0)]$$

$$T_{now}(\mathbf{x}, t) = T_{cl}(\mathbf{x}) + \sum_{m=1}^M c_m(t, z) \Phi_m(\mathbf{x})$$

$Z_s \rightarrow$ Harmonic Functions

Basis Functions (Open Boundaries)

(Chu et al., 2003 a,b JTECH)

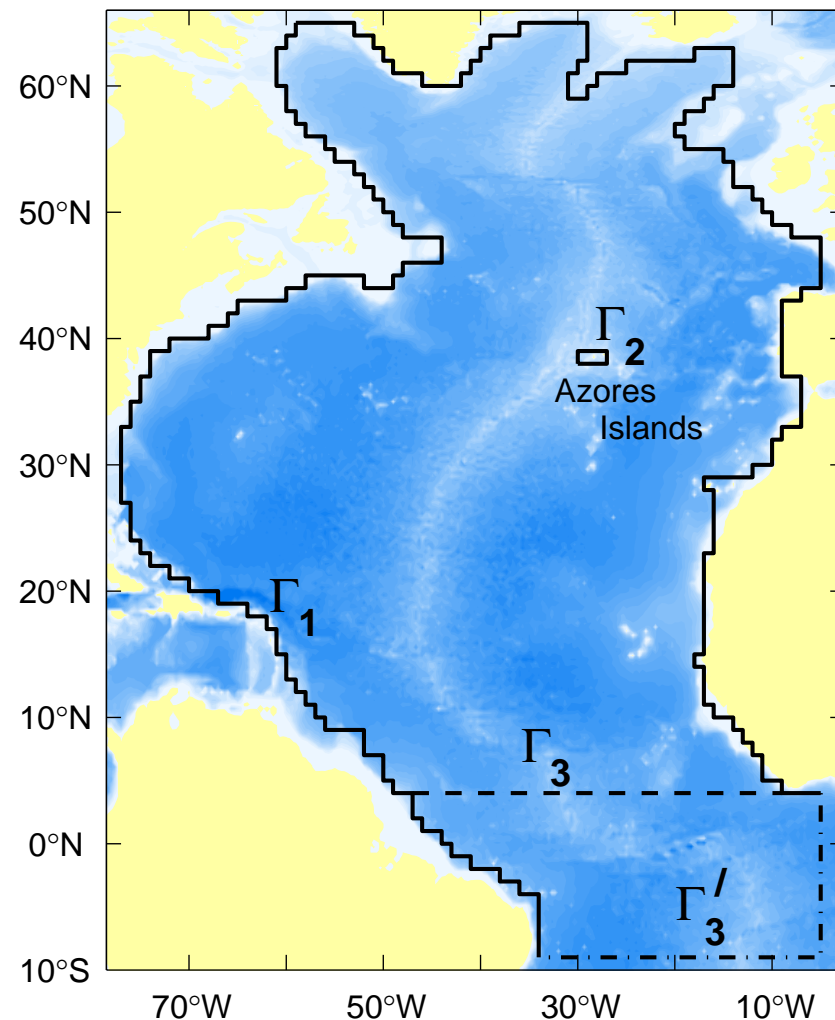
$$\Delta \Psi_k = -\lambda_k \Psi_k,$$

$$\Delta \Phi_m = -\mu_m \Phi_m,$$

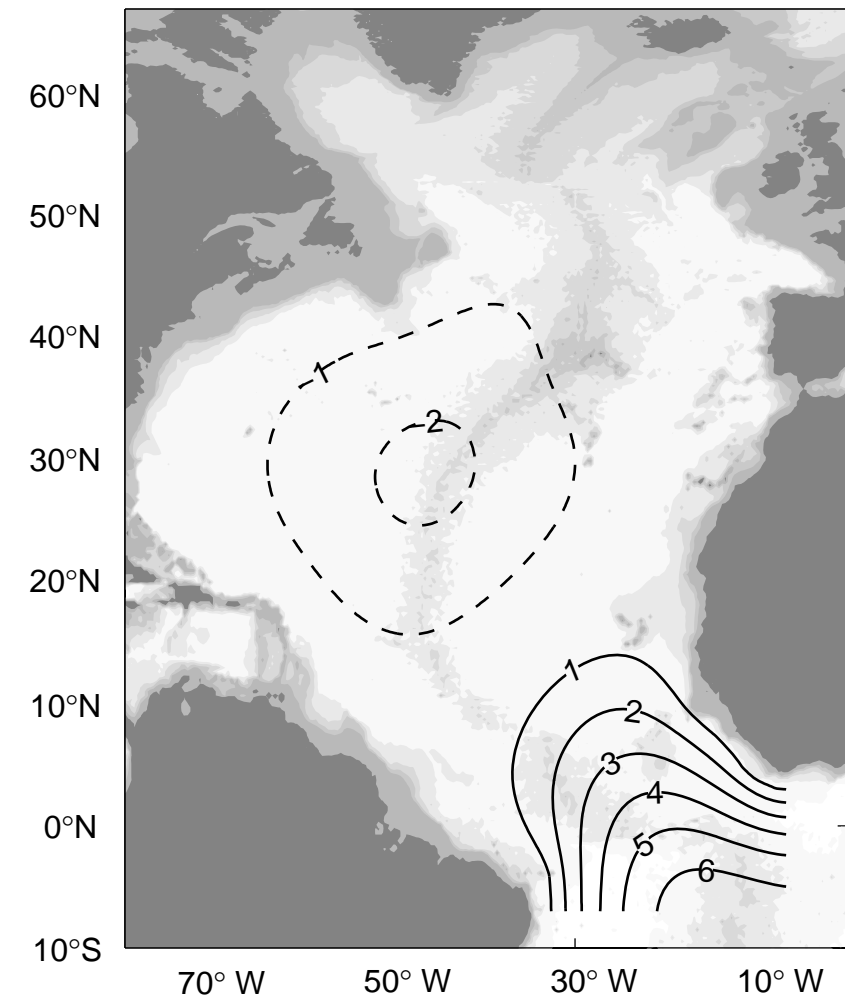
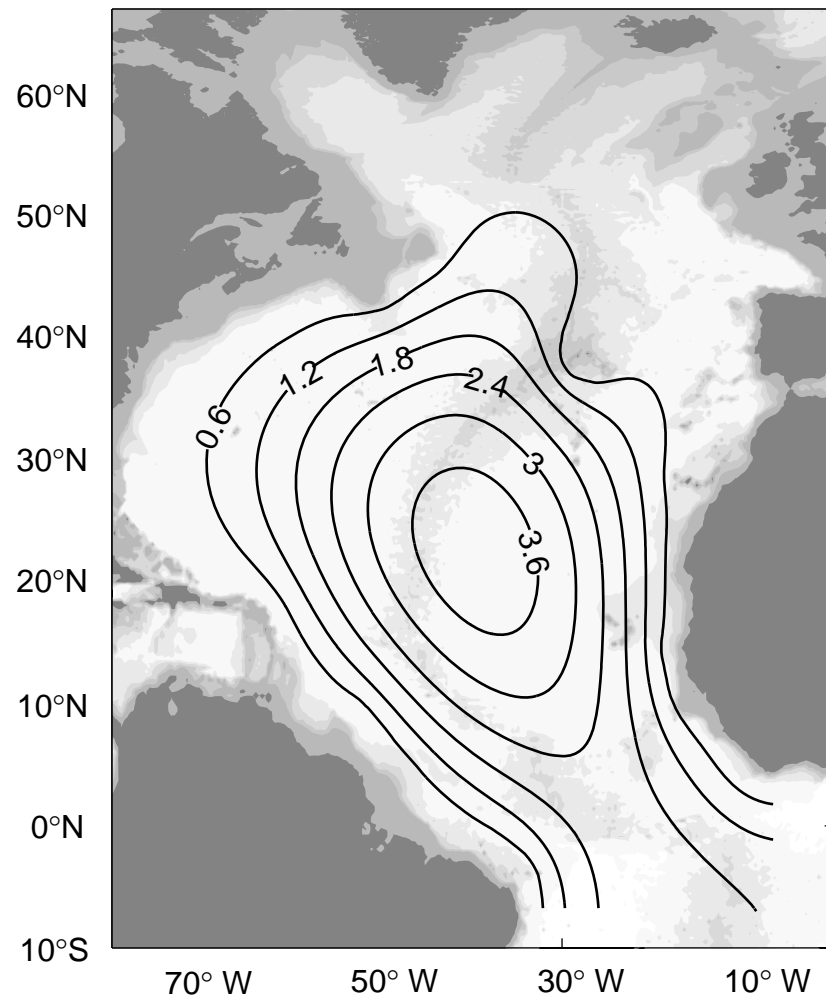
$$\Psi_k|_{\Gamma} = 0, \quad \frac{\partial \Phi_m}{\partial n}|_{\Gamma} = 0,$$

$$\left[\frac{\partial \Psi_k}{\partial n} + \kappa(\tau) \Psi_k \right] |_{\Gamma'_1} = 0, \quad \Phi_m|_{\Gamma'_1} = 0,$$

Boundary Configuration → Basis Functions for OSD

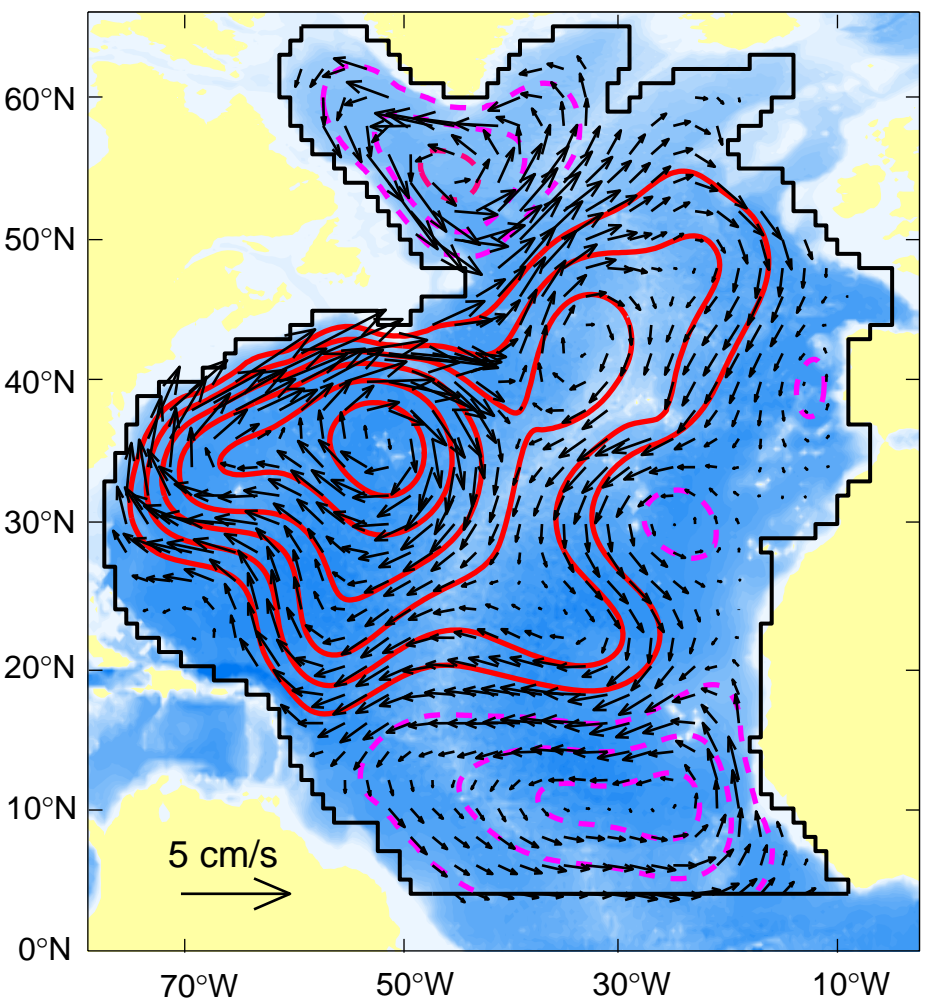
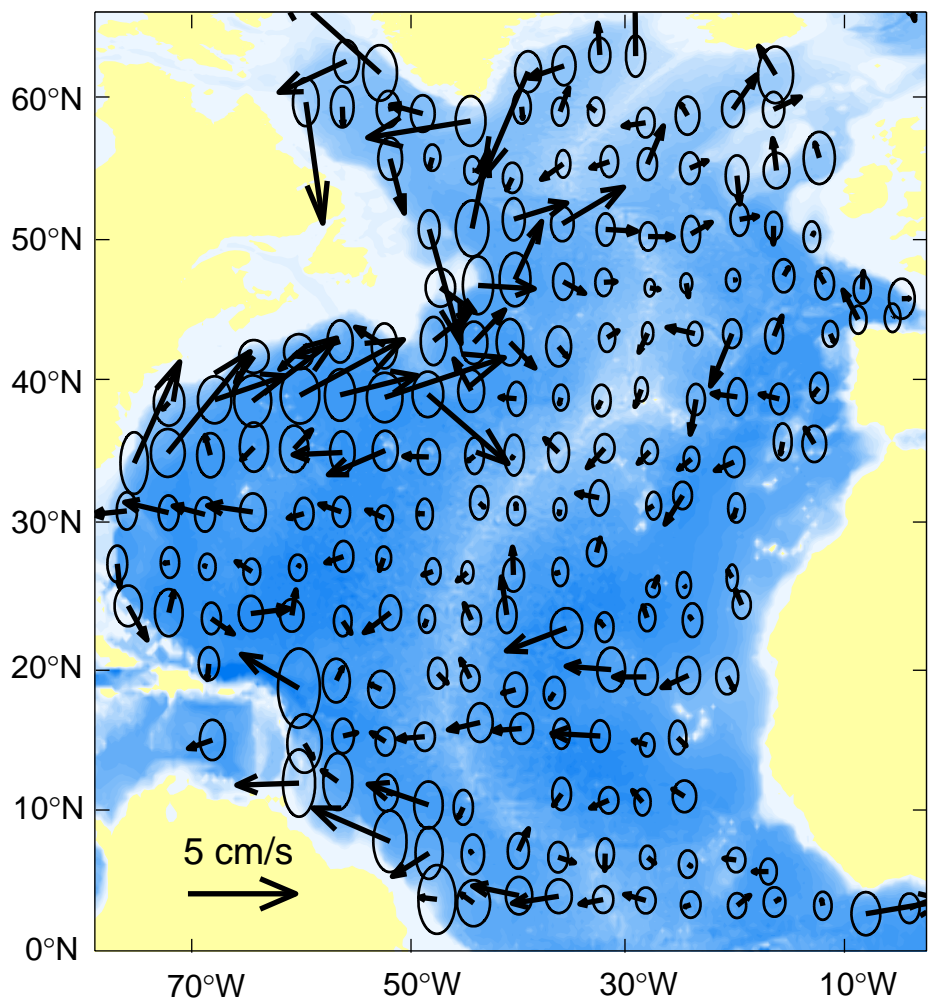


Basis Functions for Streamfunction Mode-1 and Mode-2



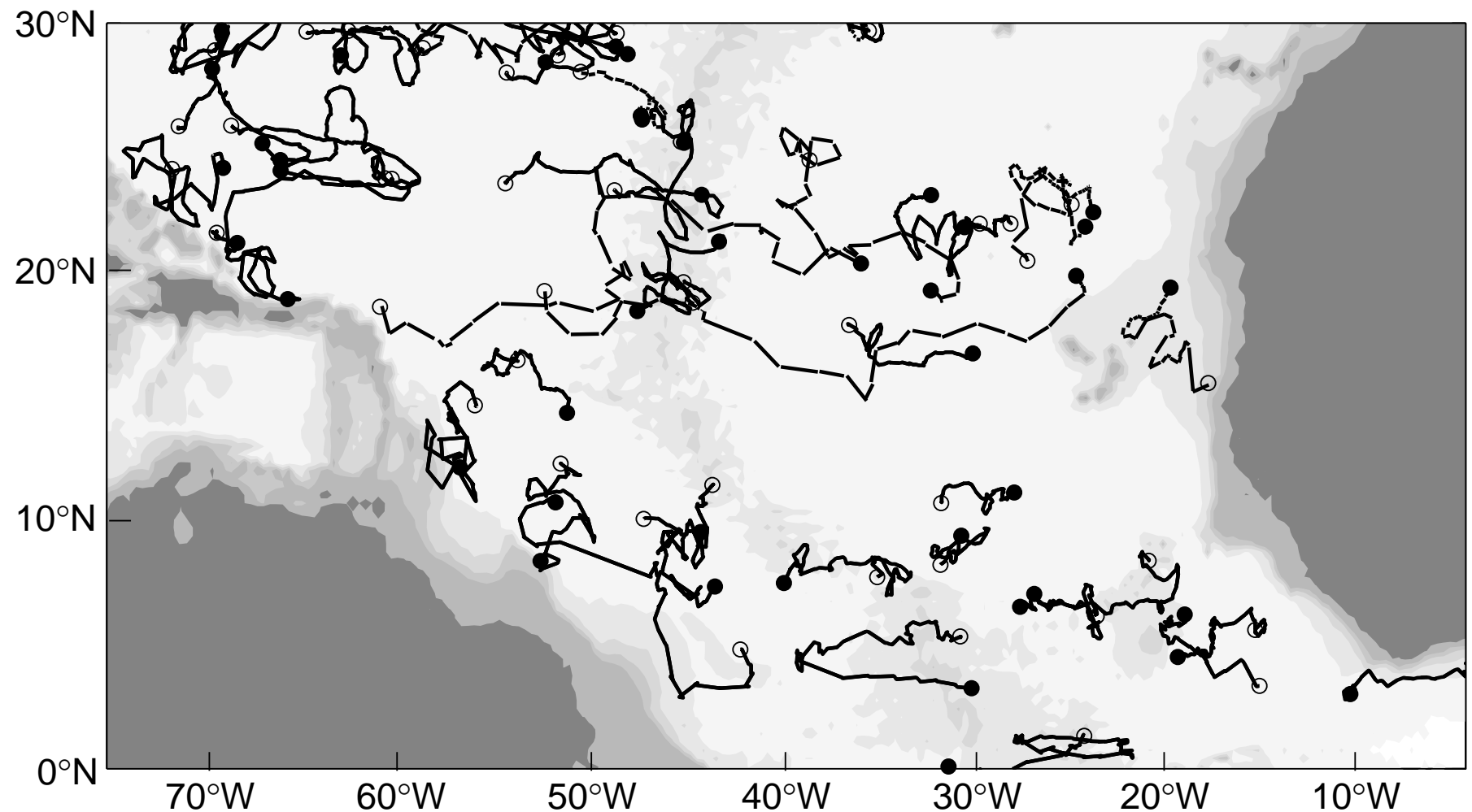
Circulations at 1000 m (March 04 to May 05)

Bin Method OSD



Baroclinic Rossby Waves in Tropical North Atlantic

Argo float tracks (with 300 days or longer drifting) at 1000 m and 1500 m (April 04-April 05)



Correction of Upper Ocean Current Drifting Caused by Vertical Shear

$$\hat{\mathbf{x}}_p = \mathbf{x}_p - \mathbf{U}_p^{eff} t_p$$

$t_p \rightarrow$ ascending/descending time (~ 10 hrs)

$$\mathbf{U}_p^{eff} = \frac{1}{H_p^0} \int_{H_p^0}^0 \mathbf{U}^*(z) dz$$

$$\mathbf{U}^* = -(\mathbf{U}_{surf} - \mathbf{U}_{now}) \frac{(z - H_p^0)}{H_p^0} + \mathbf{U}_{now}$$

Fourier Expansion → Temporal Annual and Semi-annual

$$\hat{\psi} \approx \bar{\psi}(\mathbf{x}_\perp) + \psi_1(\mathbf{x}_\perp, t) + \psi_2(\mathbf{x}_\perp, t),$$

$$\psi_1(\mathbf{x}_\perp, t) = \sum_{s=1}^2 A_{\omega_1, s} \cos(\omega_1 t + \theta_{\omega_1, s}) Z_s(\mathbf{x}_\perp) + \sum_{k=1}^{K_{opt}} B_{\omega_1, k} \cos(\omega_1 t + \vartheta_{\omega_1, k}) \Psi_k(\mathbf{x}_\perp),$$

$$\psi_2(\mathbf{x}_\perp, t) = \sum_{s=1}^2 A_{\omega_2, s} \cos(\omega_2 t + \theta_{\omega_2, s}) Z_s(\mathbf{x}_\perp) + \sum_{k=1}^{K_{opt}} B_{\omega_2, k} \cos(\omega_2 t + \vartheta_{\omega_2, k}) \Psi_k(\mathbf{x}_\perp),$$

$$T_0 = 12 \text{ months}; \quad \omega_1 = 2\pi/T_0 ; \quad \omega_2 = 4\pi/T_0$$

Fourier Expansion → Temporal Annual and Semi-annual

$$\hat{T}(\mathbf{x}_\perp, z, t) \approx \bar{T}(\mathbf{x}_\perp, z) + T_1(\mathbf{x}_\perp, z, t) + T_2(\mathbf{x}_\perp, z, t),$$

$$T_1(\mathbf{x}_\perp, z, t) = \sum_{m=1}^{M_{opt}} C_{\omega_1, m}(z) \cos[\omega_1 t + \chi_{\omega_1, m}(z)] \Xi_m(\mathbf{x}_\perp, z),$$

$$T_2(\mathbf{x}_\perp, z, t) = \sum_{m=1}^{M_{opt}} C_{\omega_2, m}(z) \cos[\omega_2 t + \chi_{\omega_2, m}(z)] \Xi_m(\mathbf{x}_\perp, z),$$

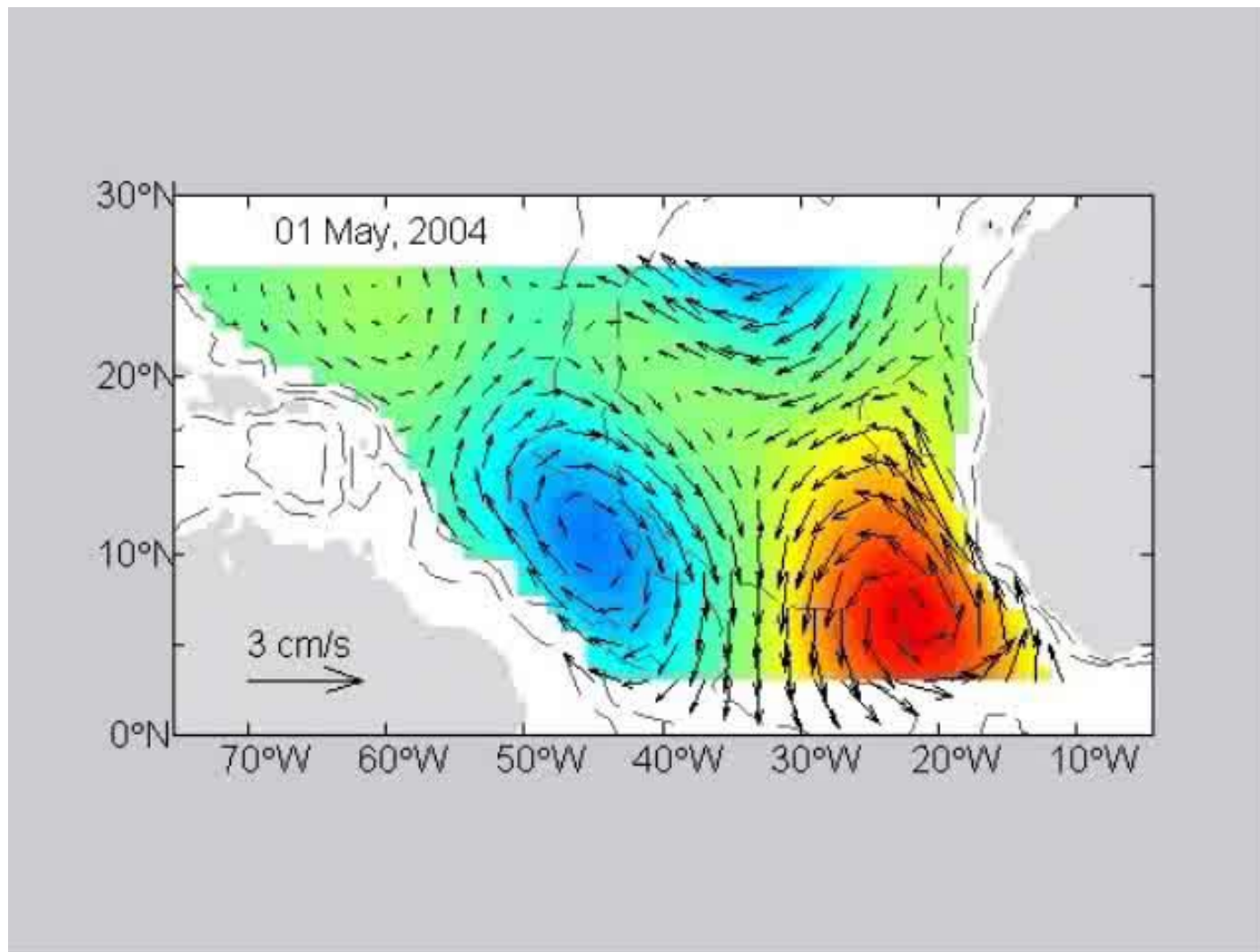
$$T_0 = 12 \text{ months}; \quad \omega_1 = 2\pi/T_0 ; \quad \omega_2 = 4\pi/T_0$$

Optimization

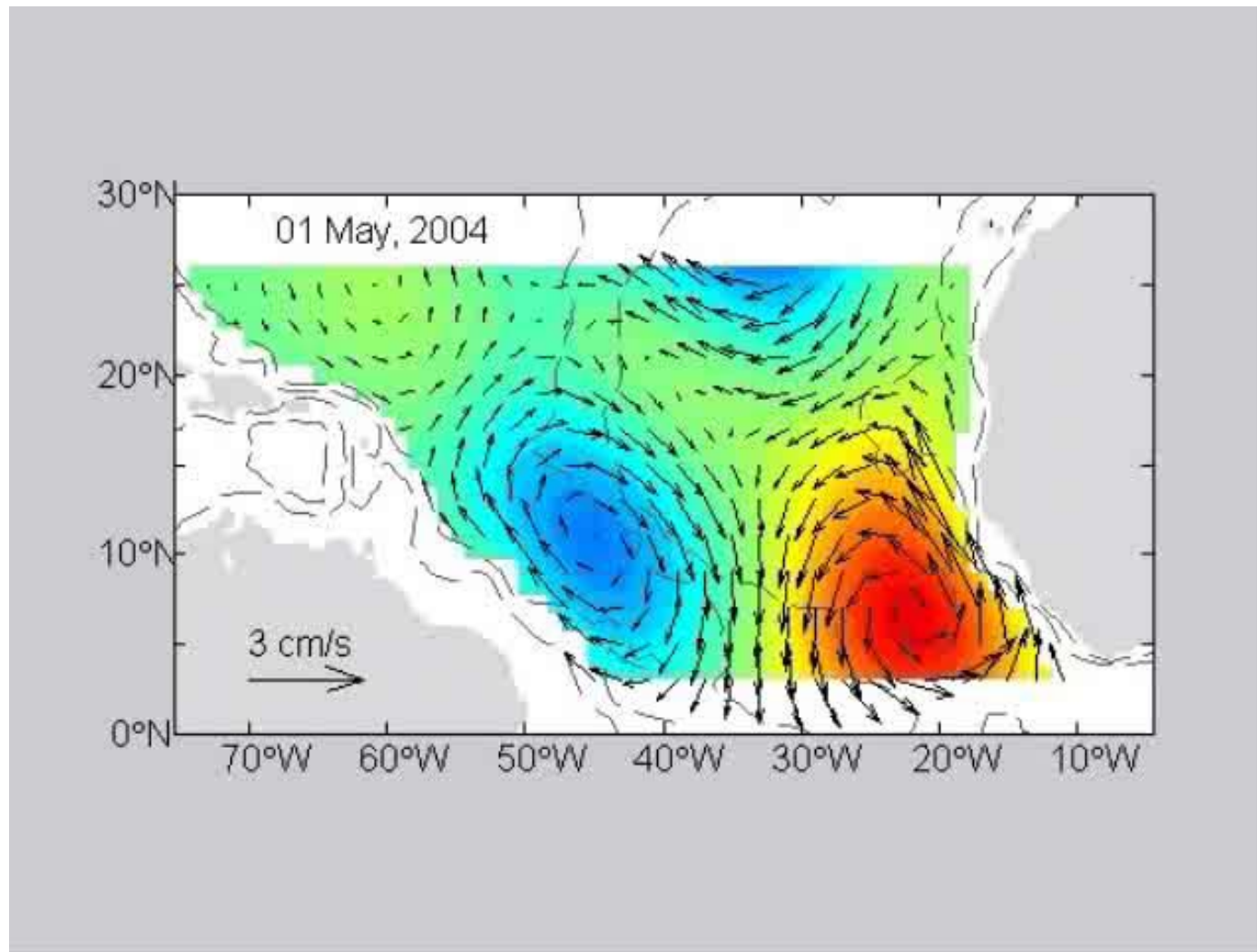
$$J_s = \int_{t_o}^{t_o + T_o} \left[a_s(t) - \sum_{\omega=\omega_1, \omega_2} A_{\omega, s} \cos(\omega t + \theta_{\omega, s}) \right]^2 dt \rightarrow \min$$

$$I_k = \int_{t_o}^{t_o + T_o} \left[b_k(t) - \sum_{\omega=\omega_1, \omega_2} B_{\omega, s} \cos(\omega t + \vartheta_{\omega, s}) \right]^2 dt \rightarrow \min$$

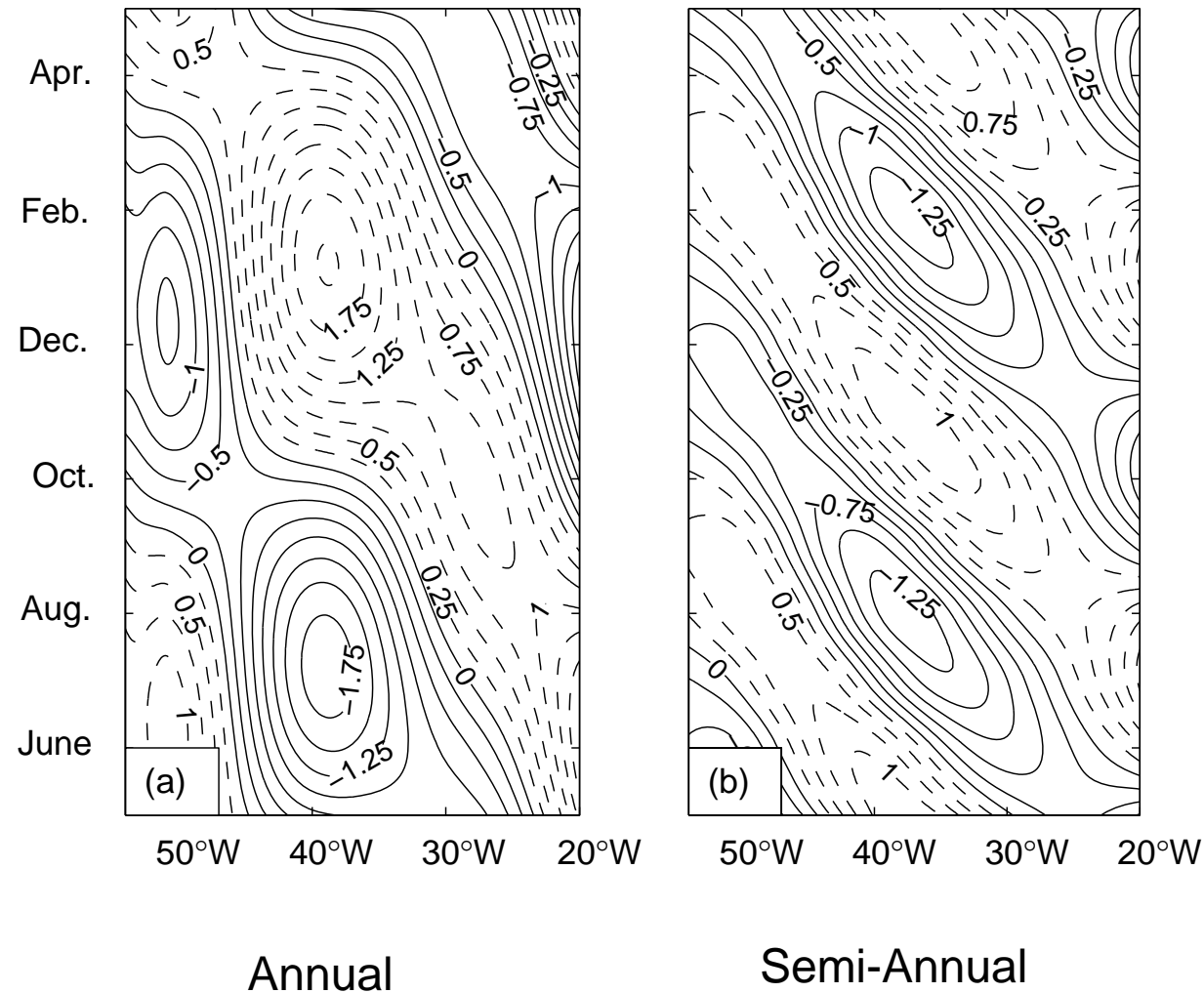
Annual Component



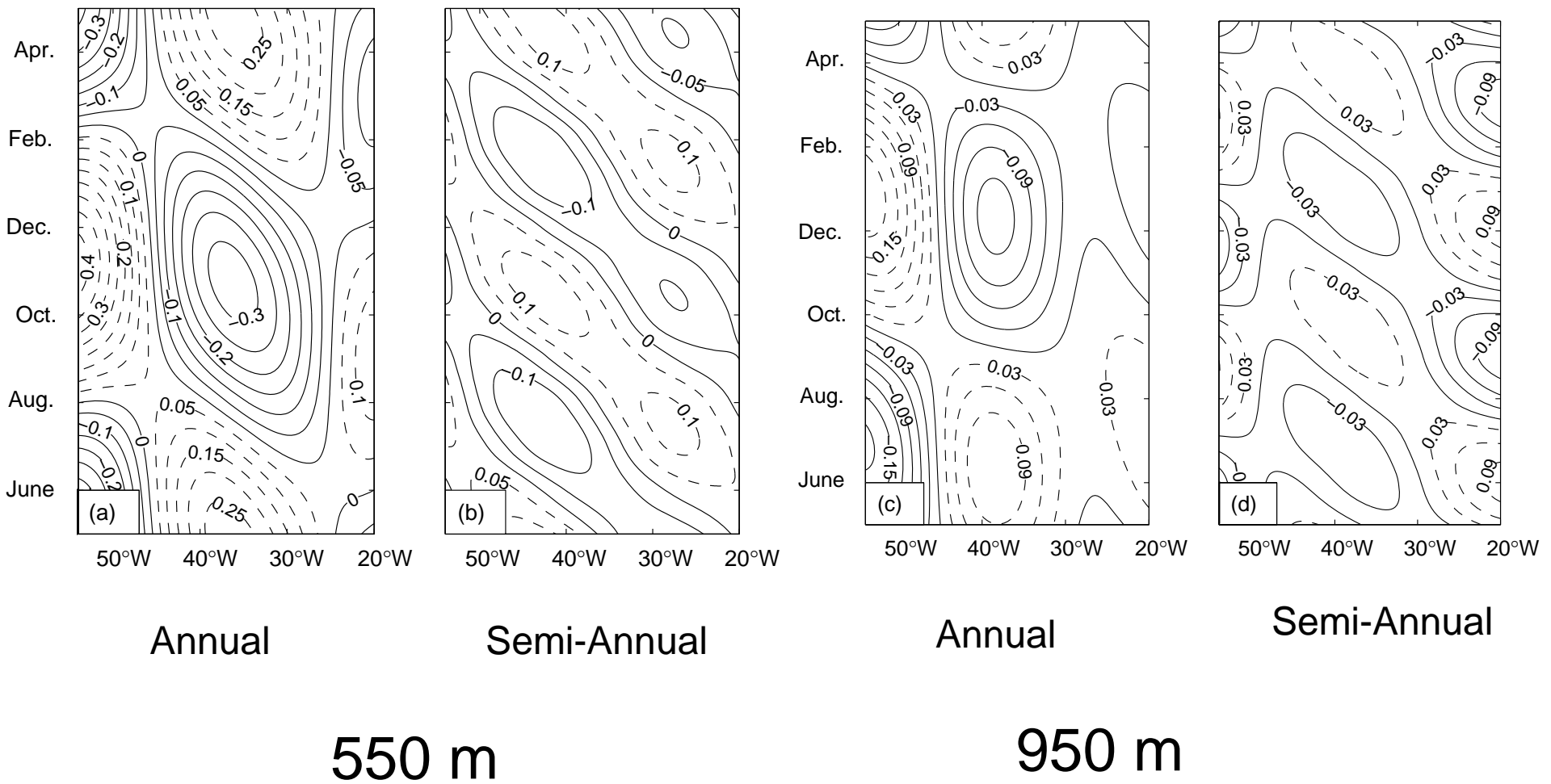
Semi-annual Component



Time –Longitude Diagrams of Meridional Velocity Along 11°N

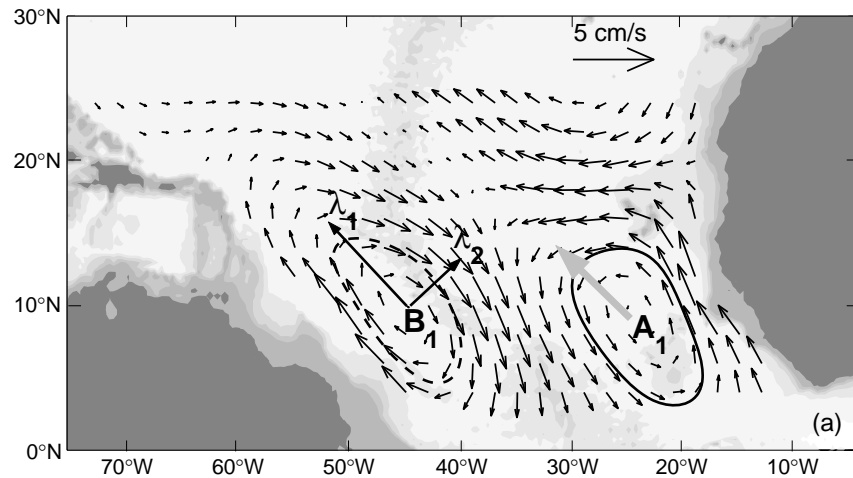


Time –Longitude Diagrams of temperature Along 11°N

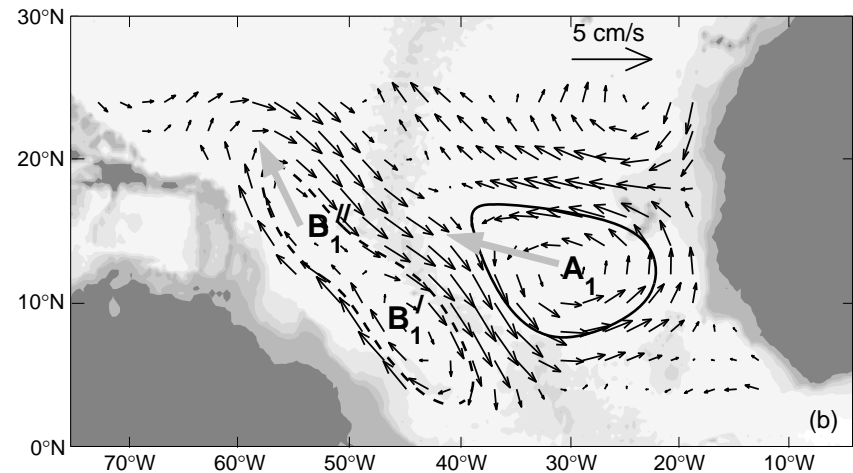


Annual Currents (1000 m)

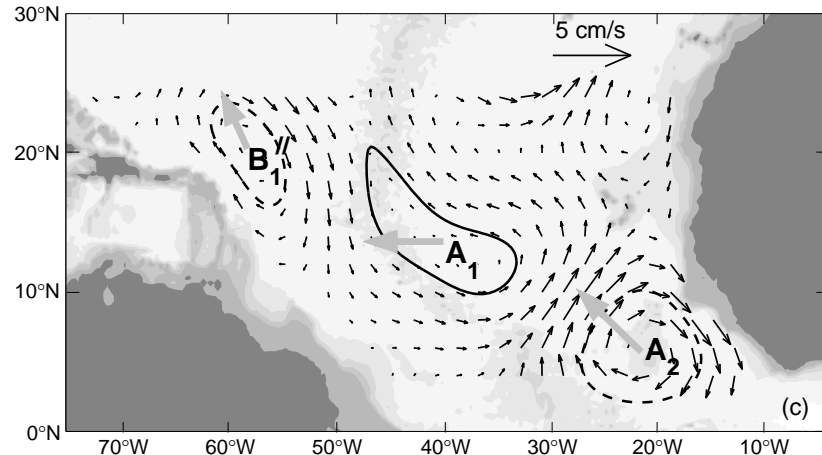
May-Jun 2004



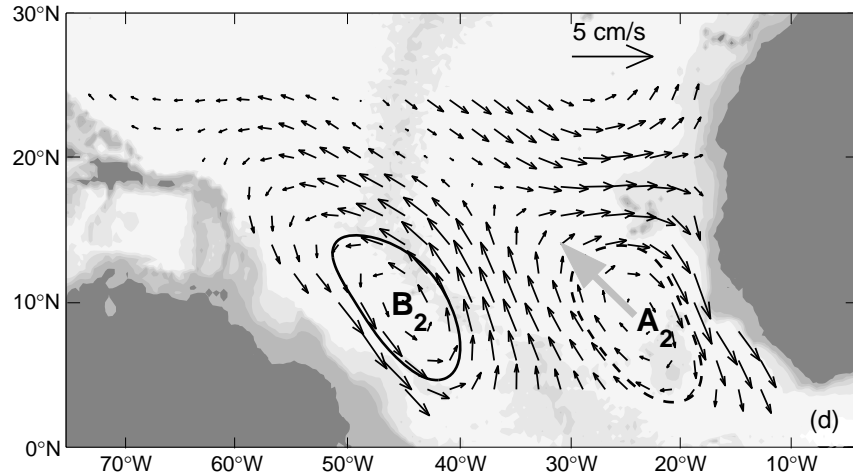
Jul-Aug 2004



Sep-Oct 2004



Nov-Dec 2004



Characteristics of Annual Rossby Waves

| Latitude | March, 04 – May, 05 float data | | | March, 04 – May, 06 float data | | |
|----------|-----------------------------------|------------|------------|-----------------------------------|------------|------------|
| | c_p (cm/s) | L_1 (km) | L_2 (km) | c_p (cm/s) | L_1 (km) | L_2 (km) |
| 5°N | 12 | 1200 | 1100 | 12 | 1300 | 900 |
| 8°N | 16 | 2500 | 1400 | 12 | 2100 | 1100 |
| 11°N | 14 | 2200 | 1400 | 11 | 1900 | 1100 |
| 13°N | 11 | 2100 | 1500 | 10 | 2300 | 1500 |

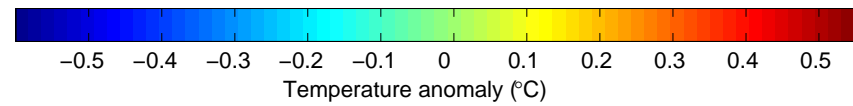
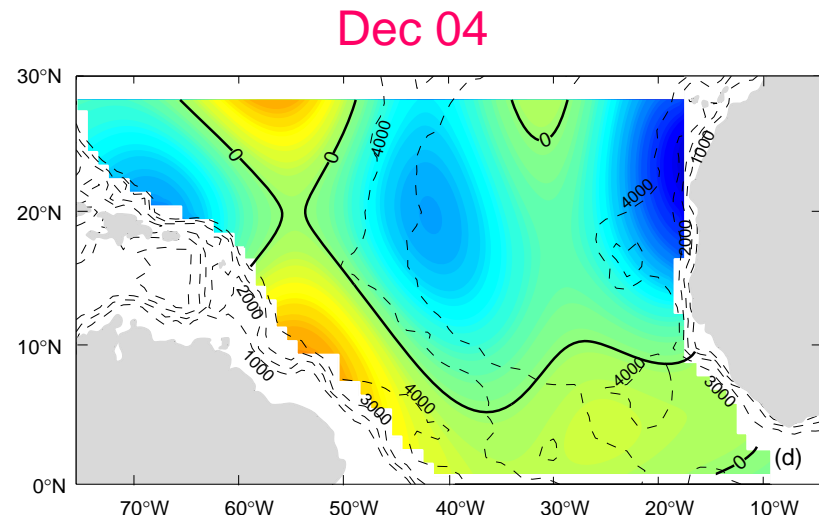
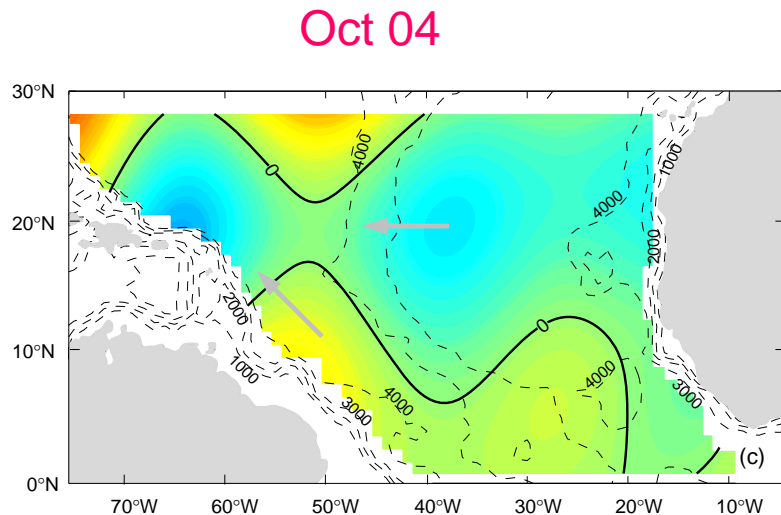
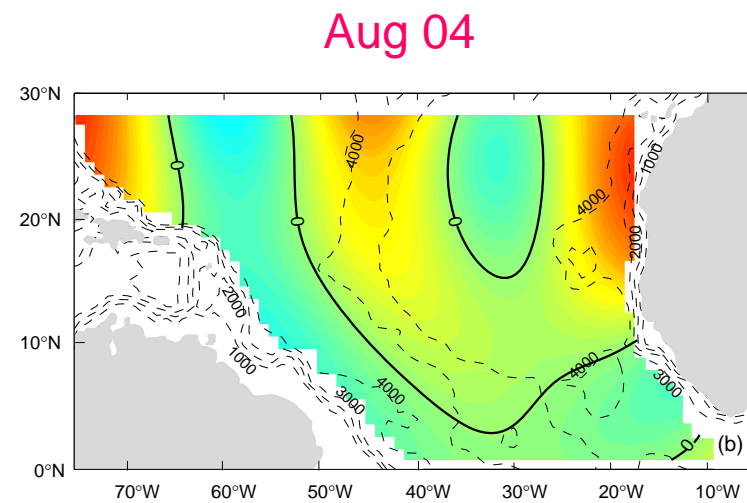
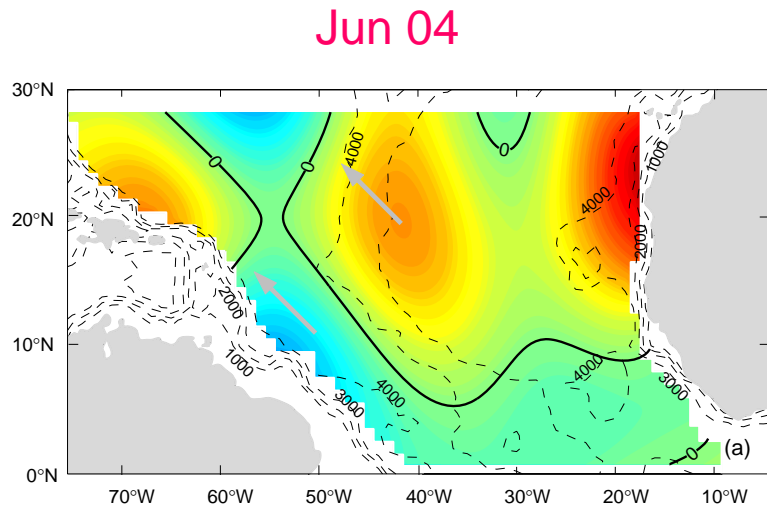
Western
Basin

Eastern
Basin

Western
Basin

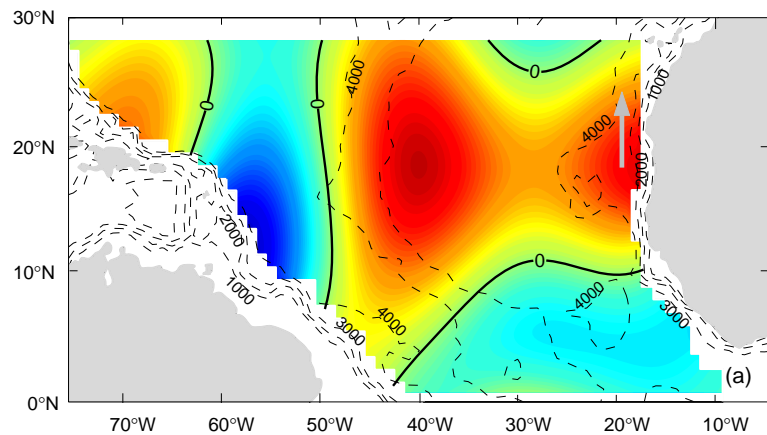
Eastern
Basin

Annual Monthly Temperature Anomaly ($^{\circ}\text{C}$) at 950 m Depth → Annual Rossby Waves (7-10 cm/s)

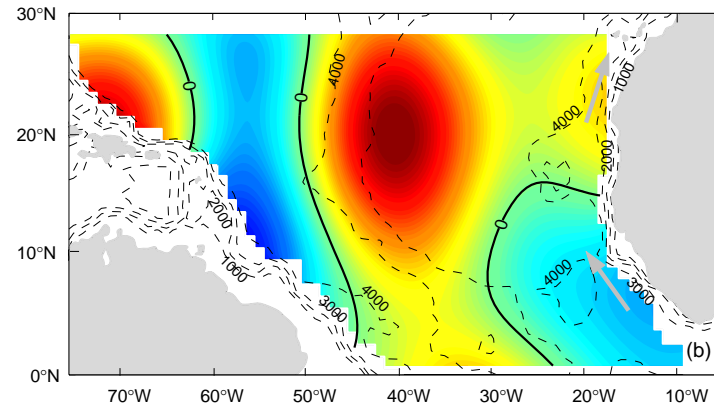


Annual Monthly Temperature Anomaly ($^{\circ}\text{C}$) at 250 m Depth → Equatorially Forced Coastal Kelvin waves (27-30 cm/s)

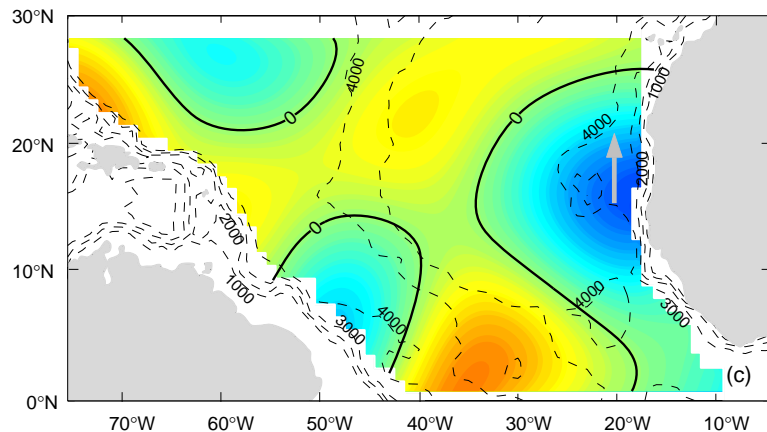
Jun 04



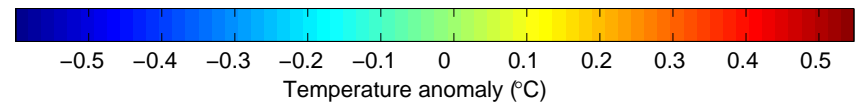
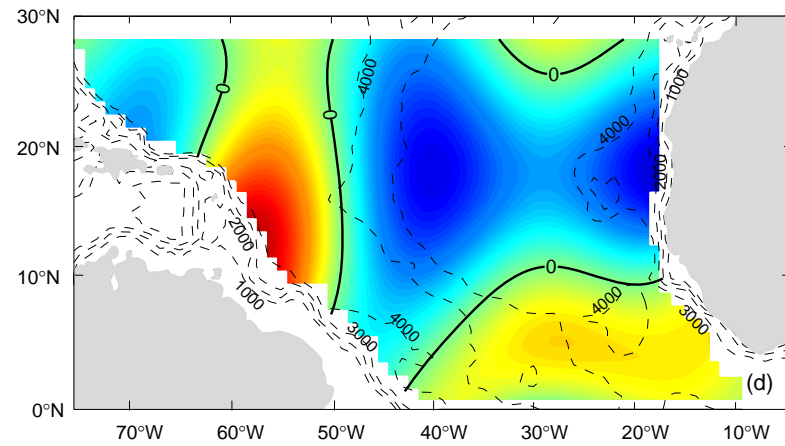
Aug 04



Oct 04

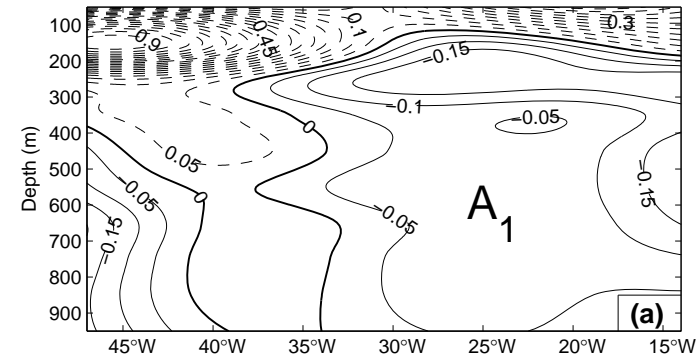


Dec 04

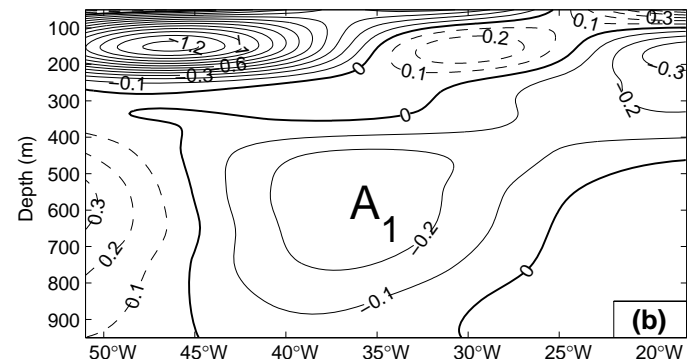


Zonal cross-sections of the annual component of the temperature anomaly ($^{\circ}\text{C}$)

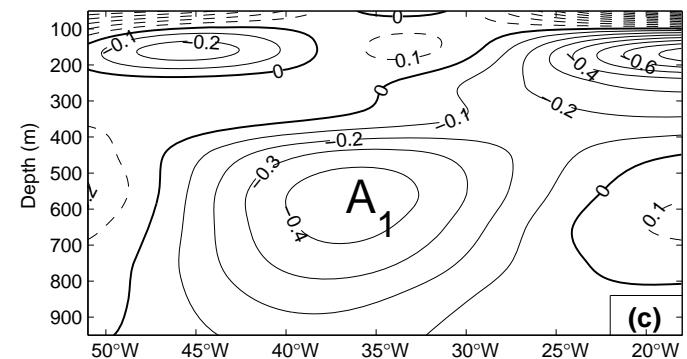
6°N in Jun 04 →



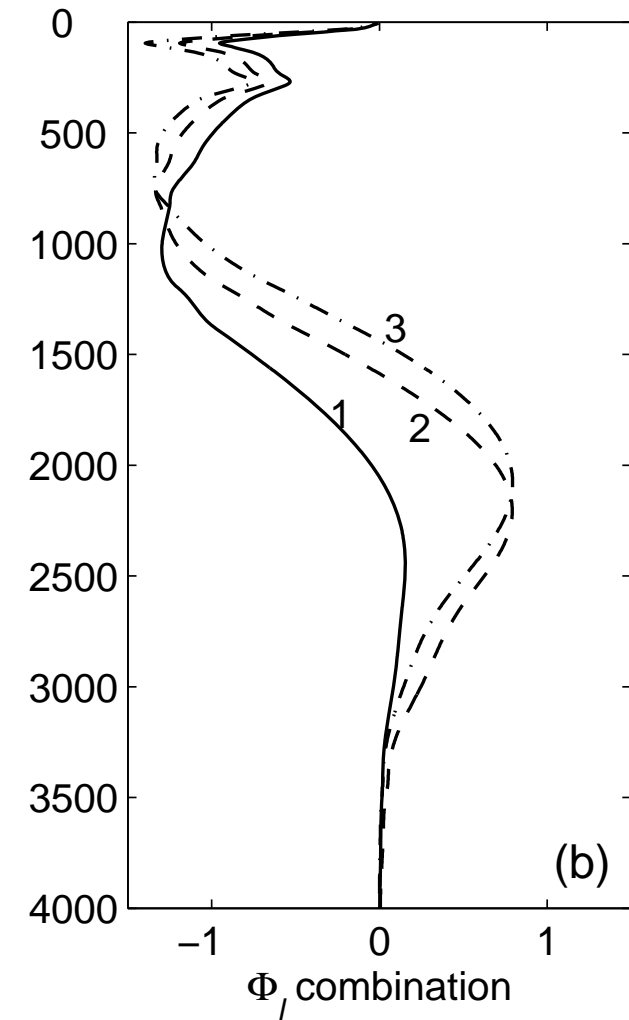
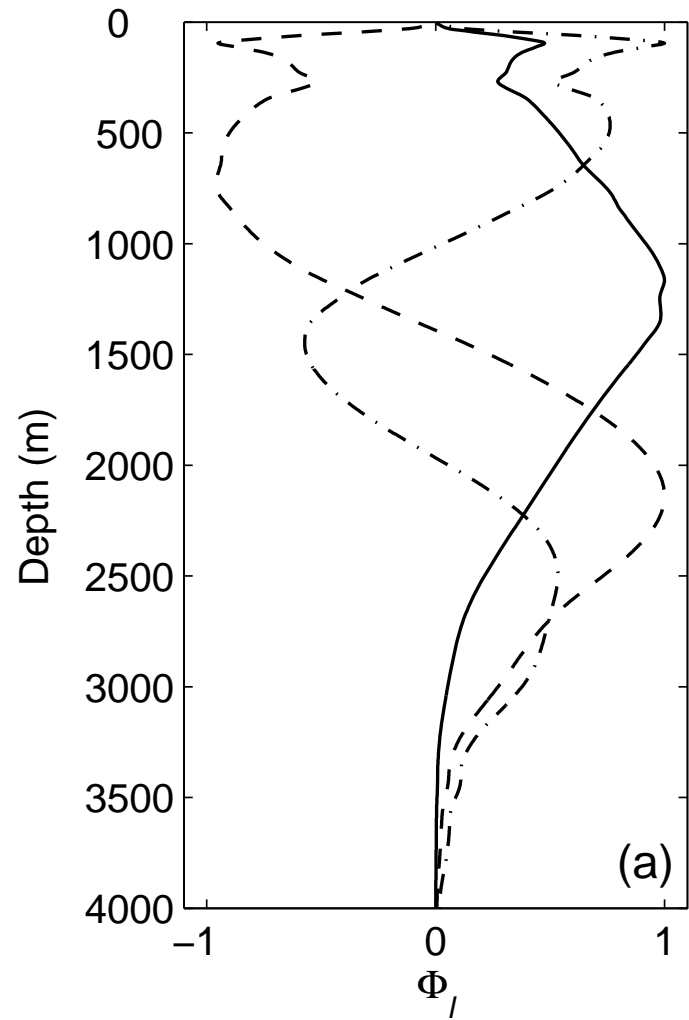
11°N in Oct, 04 →



16°N in Oct 04 →



Baroclinic Modes



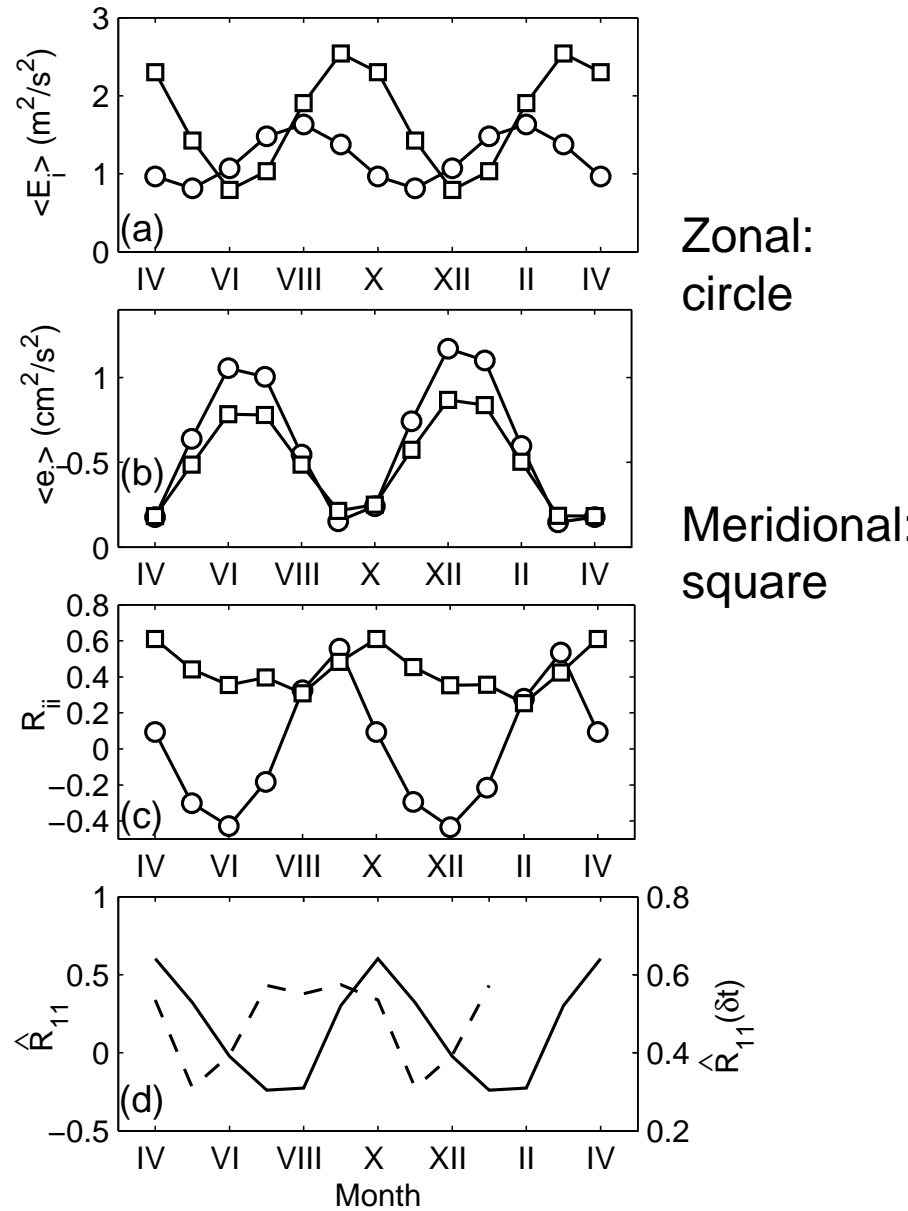
Annual Component in the Western Sub-Basin

Mean wind KE

Mean KE for mid-depth currents

Correlation between Winds and currents

Correlation between wind Stress curl and streamfunction
(solid: no-lag, dashed: 3 mon lag)



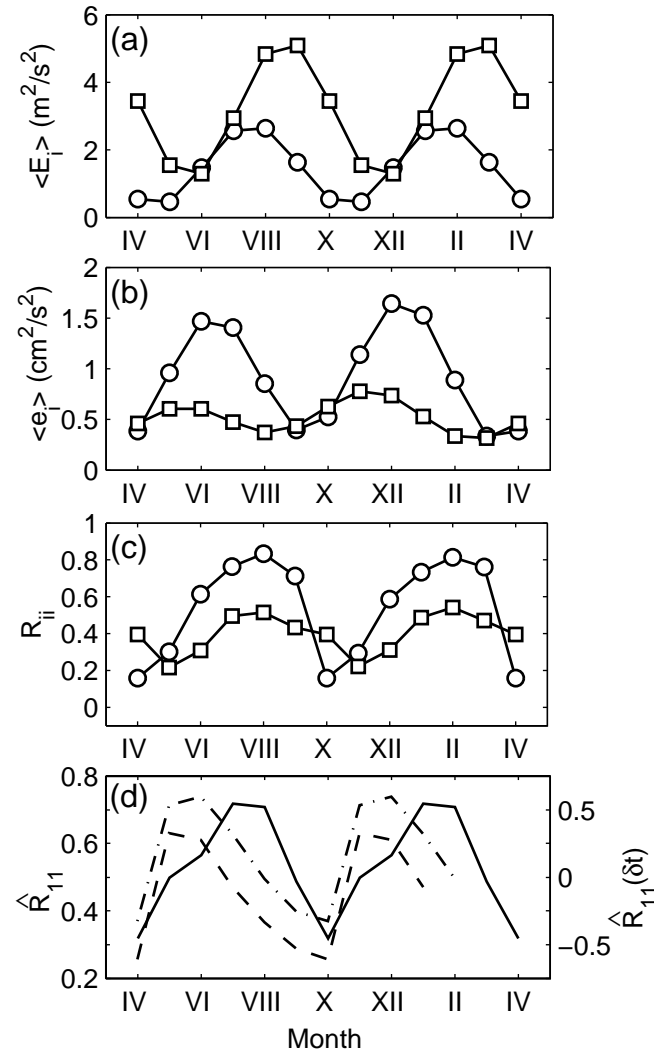
Annual Component in the Eastern Sub-Basin

Mean wind KE

Mean KE for mid-depth currents

Correlation between Winds and currents

Correlation between wind Stress curl and streamfunction
(solid: no-lag, dashed: 3 mon lag)

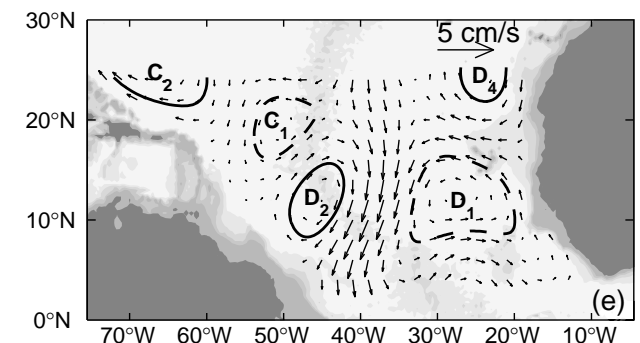
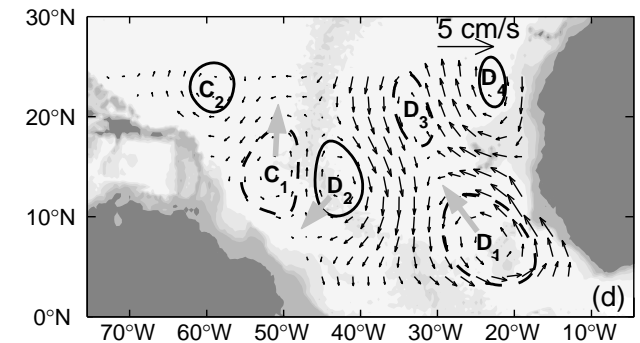
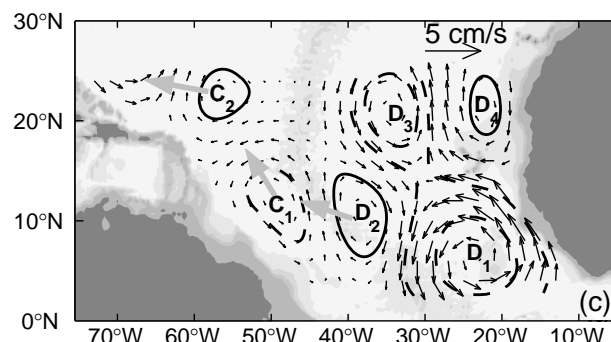
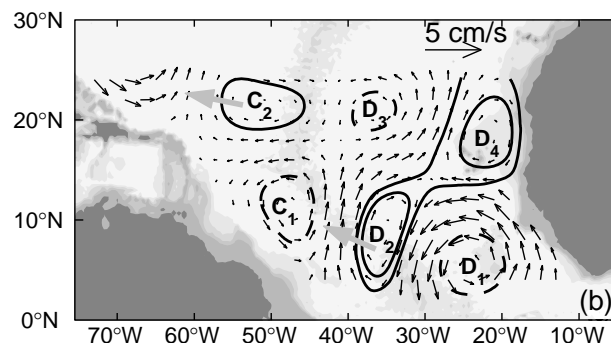
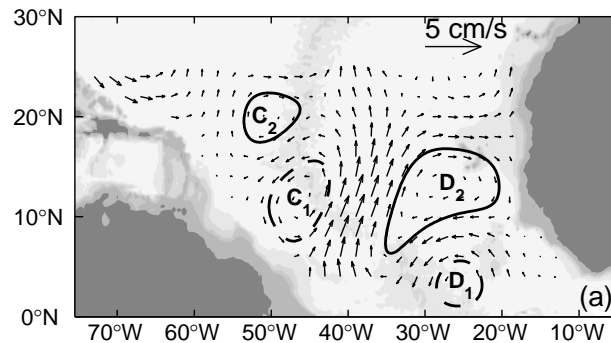


Zonal:
circle

Meridional:
square

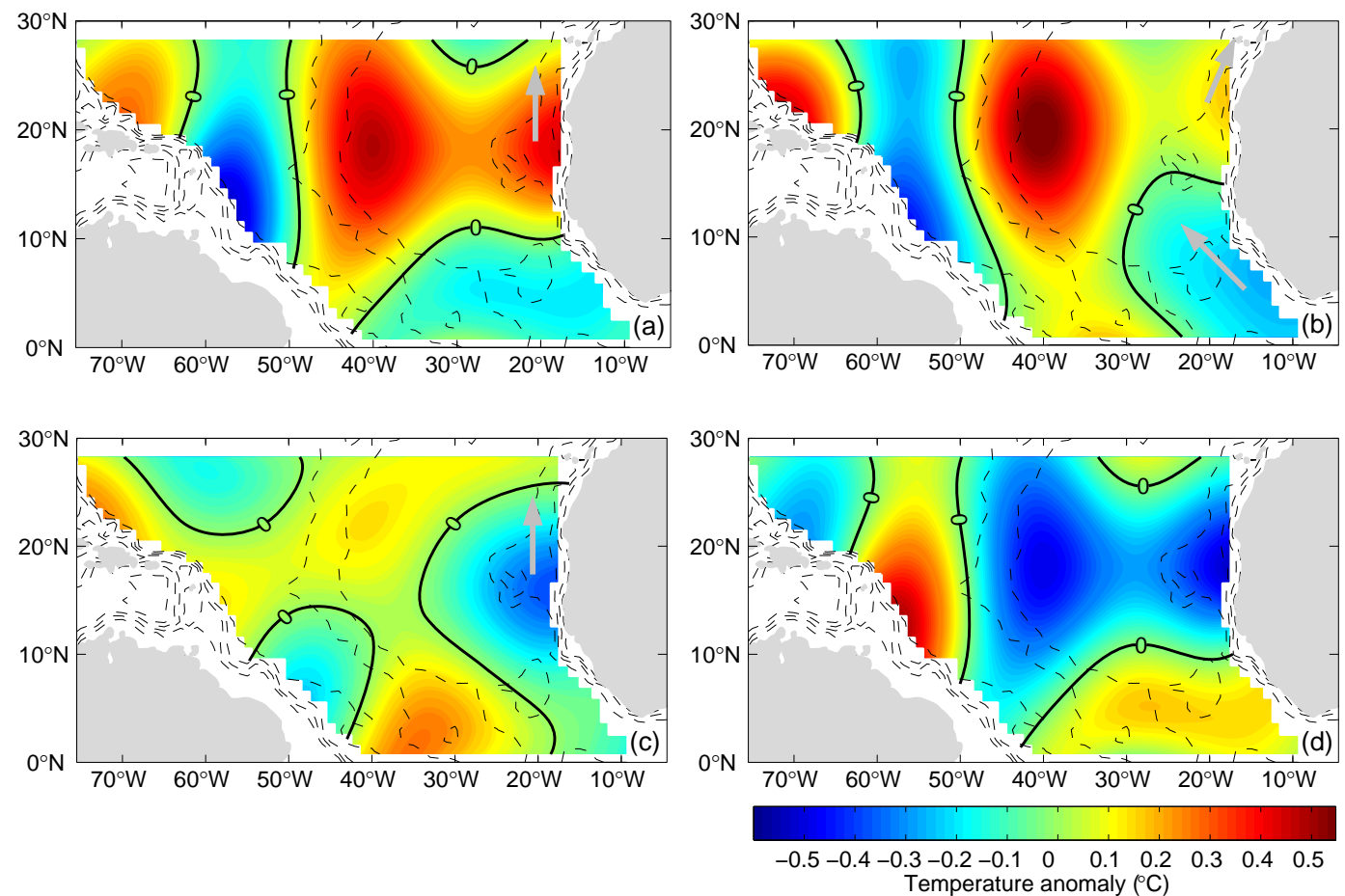
Semi-annual currents at 1000 m depth (2004)

- (a) 5/15**
- (b) 5/30**
- (c) 6/14**
- (d) 6/29**
- (e) 7/13**



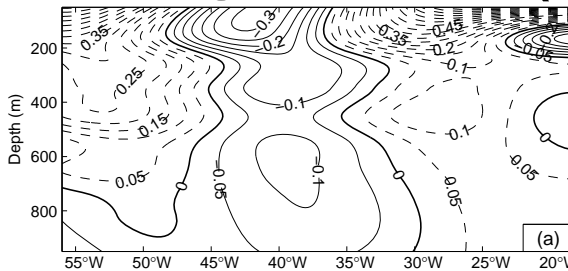
Semi-annual monthly temperature anomaly at 950m depth

- (a) Jun 04
- (b) Aug 04
- (c) Oct 04
- (d) Dec 04.

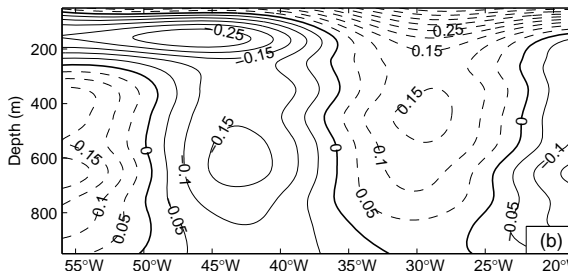


Semi-annual component of monthly temperature anomaly along 11°N (2004)

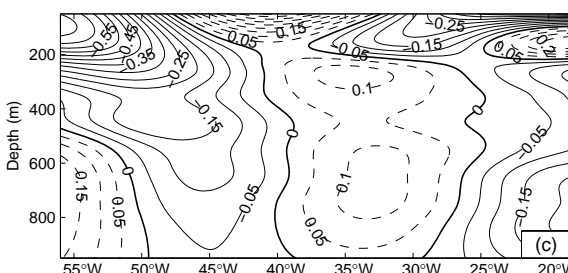
(a) 6/4



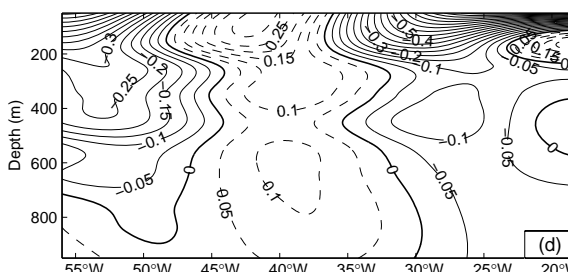
(b) 7/4



(c) 8/4

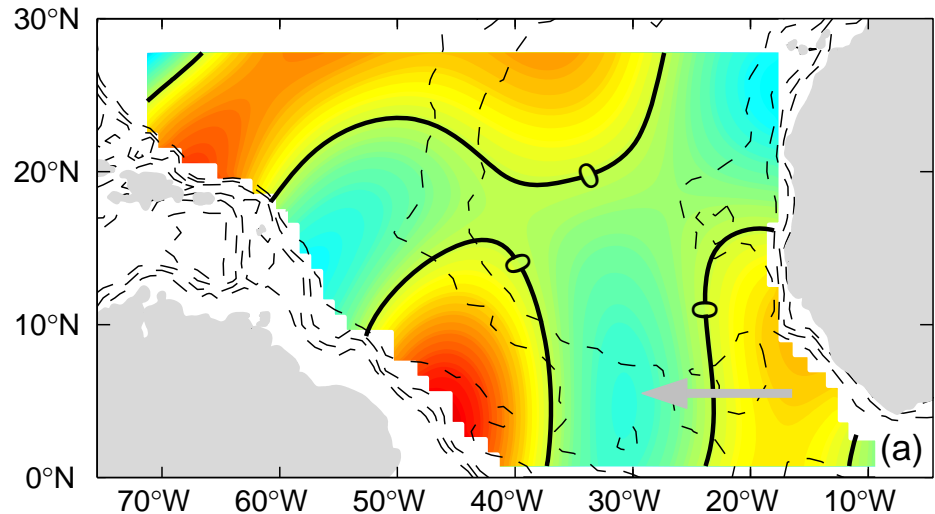


(d) 9/4

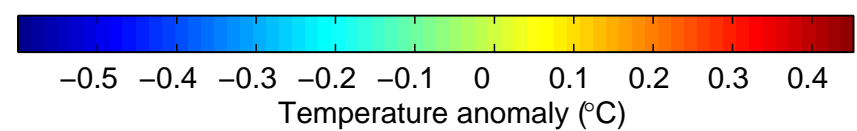
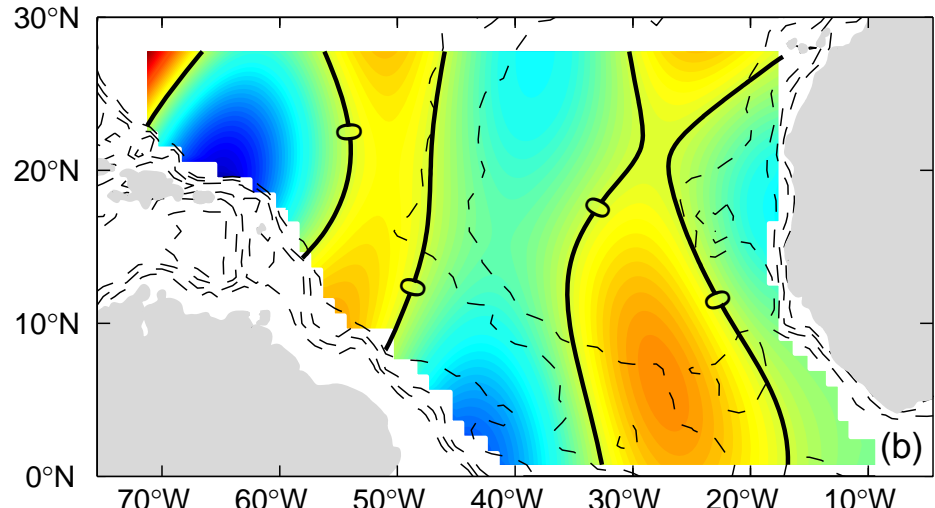


Semi-annual temperature anomaly at 550m depth (2004)

(a) 5/15

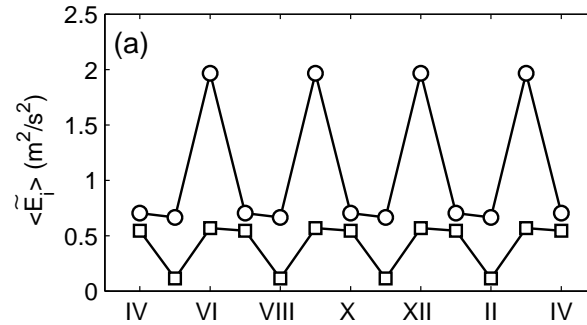


(b) 6/29

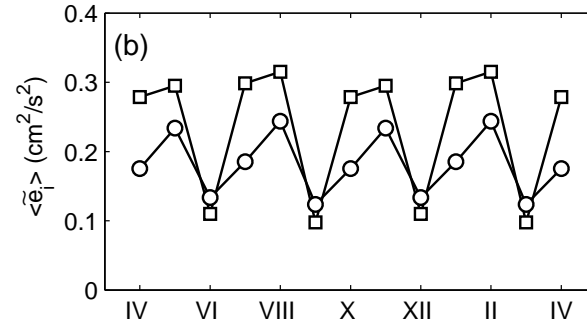


Semiannual Component in the Western Sub-Basin

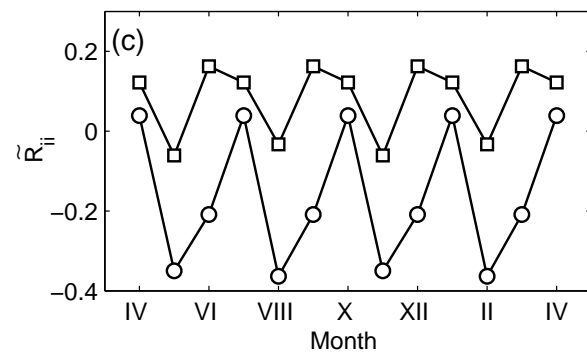
(a) wind KE



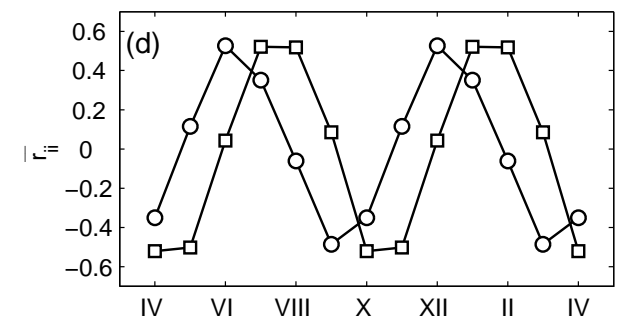
(b) current KE



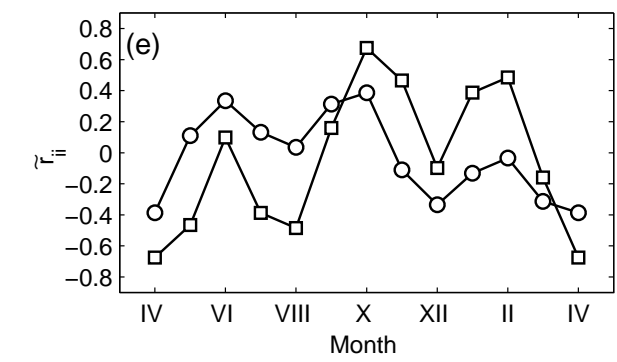
(c) corr wind
stress and currents



(d) corr between
semi-annual currents
and annual mean wind

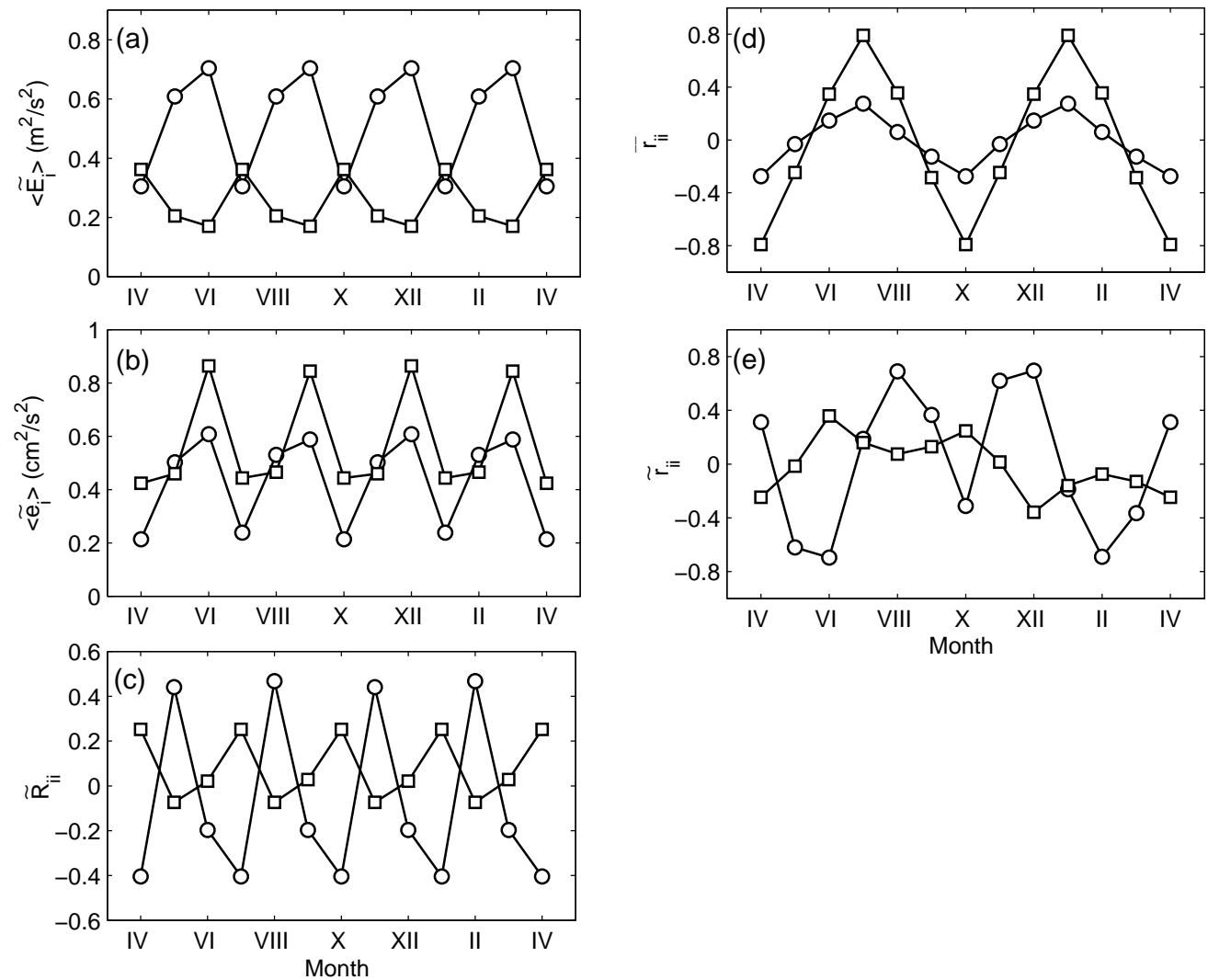


(e) corr between
semiannual currents
and annual wind stress.



Semiannual Component in the Eastern Sub-Basin

- (a) wind KE
- (b) current KE
- (c) corr wind stress and currents
- (d) corr between semi-annual currents and annual mean wind
- (e) corr between semiannual currents and annual wind stress.



Results

- Mid-depth Rossby waves are identified using the Argo data.
- The annual and semi-annual Rossby waves are detected in both the western and eastern sub-basins.
- The wind-driven Ekman pumping seems to be responsible for the Rossby wave generation in both the sub-basins.